Molecules and Cells

The Molecular Mechanism of Long Non-Coding RNA MALAT1-Mediated Regulation of Chondrocyte Pyroptosis in Ankylosing Spondylitis

Wei Chen[1], Feilong Wang[1], Jiangtao Wang[1], Fuyu Chen[1], and Ting Chen[2,*]

[1]Department of Orthopaedics, The First People's Hospital of Yongkang, Affiliated to Hangzhou Medical College, Jinhua 321300, China, [2]Department of Pediatric Orthopaedic, Xinhua Hospital Affiliated to Shanghai Jiaotong University School of Medicine, Shanghai 200092, China
*Correspondence: chenting@xinhuamed.com.cn
https://doi.org/10.14348/molcells.2022.2081
www.molcells.org

Long non-coding RNAs (lncRNAs) may be important regulators in the progression of ankylosing spondylitis (AS). The competing endogenous RNA (ceRNA) activity of lncRNAs plays crucial roles in osteogenesis. We identified the mechanism of the differentially expressed lncRNA MALAT1 in AS using bioinformatic analysis and its ceRNA mechanism. The interaction of MALAT1, microRNA-558, and GSDMD was identified using integrated bioinformatics analysis and validated. Loss- and gain-of-function assays evaluated their effects on the viability, apoptosis, pyroptosis and inflammation of chondrocytes in AS. We found elevated MALAT1 and GSDMD but reduced miR-558 in AS cartilage tissues and chondrocytes. MALAT1 contributed to the suppression of cell viability and facilitated apoptosis and pyroptosis in AS chondrocytes. GSDMD was a potential target gene of miR-558. Depletion of MALAT1 expression elevated miR-558 by inhibiting GSDMD to enhance cell viability and inhibit inflammation, apoptosis and pyroptosis of chondrocytes in AS. In summary, our key findings demonstrated that knockdown of MALAT1 served as a potential suppressor of AS by upregulating miR-558 via the downregulation of GSDMD expression.

Keywords: ankylosing spondylitis, chondrocyte, gasdermin D, metastasis-associated lung adenocarcinoma transcript 1, microRNA-558, pyroptosis

INTRODUCTION

Ankylosing spondylitis (AS) is a chronic immune-regulated inflammatory disease that primarily affects the axial and sacroiliac skeleton (Garcia-Montoya et al., 2018). AS affects the peripheral joints, eyes, or bowel and elevates the risk of cardiovascular or pulmonary manifestations in approximately 0.1% of the population worldwide (Wenker and Quint, 2021). Considerable conventional methods, including clinical symptoms and imaging techniques, are available in AS treatments and its relevant inflammatory spondylitis (Xi et al., 2019). However, there is an urgent need to develop cost-effective treatments for AS. Pyroptosis is an inflammatory type of regulated cell death that occurs following inflammasome activation (McKenzie et al., 2020). Activated pyroptosis causes in vivo inflammatory responses that lead to different inflammatory disease pathologies (Liu and Lieberman, 2017). Therefore, the underlying mechanisms mediating AS pyroptosis should be elucidated to identify novel therapeutic targets for AS treatment.

Noncoding regions represent 98% of the entire human genome and include intergenic, intronic, and non-coding genes

Received 9 September, 2021; revised 18 December, 2021; accepted 26 December, 2021; published online 9 June, 2022

eISSN: 0219-1032

(Li et al., 2019). Long non-coding RNAs (lncRNAs) function in many cell processes, including apoptosis and pyroptosis (He et al., 2020) and regulate inflammatory immune responses in many autoimmune diseases, including AS (Huang et al., 2021). MALAT1 is a 6.5 kb nuclear-residing lncRNA that has emerged as a regulator of inflammatory factor production (Puthanveetil et al., 2015). The involvement of MALAT1 in pyroptosis in different diseases has been reported (Han et al., 2018; Liu et al., 2020). However, the pathological functions of MALAT1 in AS are not known. Differentially expressed lncRNAs bind to microRNAs (miRNAs), which suggests their role in the pathogenesis of AS (Tay et al., 2014; Zhang et al., 2017). MiRNAs are small noncoding RNA molecules that primarily act as biomarkers in various activities, including the pathogenesis and prognosis of AS (Mohammadi et al., 2018). Decreased miR-558 was observed in human osteoarthritis chondrocytes (Park et al., 2013), but its role in AS is not clear. Gasdermin D (GSDMD) is a substrate of caspase-1, and it is implicated in pyroptosis and secretion of the inflammatory element interleukin (IL)-1β (He et al., 2015). One study suggested that the knockdown of GSDMD inhibited pyroptosis via cytosolic lipopolysaccharide and known canonical inflammasome ligands (Shi et al., 2015). Recent studies showed that MALAT1 protected cardiomyocytes from isoproterenol-induced apoptosis by binding to miR-558 to promote ULK1-dependent autophagy (Guo et al., 2019). Considering the above-described effects, we hypothesized the existence of a specific relationship between MALAT1, miR-558, and *GSDMD* in pyroptosis in AS. We analyzed these factors in a series of experiments.

MATERIALS AND METHODS

Bioinformatics analysis

The AS-related gene expression dataset GSE41038 was deposited from the Gene Expression Omnibus (GEO) database, including 4 normal cartilage tissue samples and 2 AS tissue samples. The R language affy package was used for pre-treatment normalization of the expression data. The differentially expressed genes were obtained using the limma package with $P < 0.05$. The miRNAs with possible binding sites with lncRNAs were predicted in the RNA22 database. MRNA possible binding sites with miRNAs were predicted using the TargetScan website. The intersection of binding sites between lncRNA and mRNA was obtained using jvenn, followed by construction of a Venn diagram.

Study subjects

AS cartilage tissues in the hip joint were collected from 22 patients with AS (17 males and 5 females; age, 20-46 years with a mean age of 29 years) who underwent hip replacement (n = 8) and patients who underwent biopsy (n = 14) by needle puncture in the Department of Orthopedic Surgery and Orthopedics of Xinhua Hospital Affiliated to Shanghai Jiaotong University School of Medicine from April 2012 to August 2016. A total of 18 control specimens (11 males and 7 females; age, 22-39 years with a mean age of 30 years) were obtained from traumatic femoral head fracture or hip fracture surgery. After separation, the specimens were fixed in 4% paraformaldehyde at 4°C for 2-4 h, followed by incubation in phosphate-buffered saline (PBS) containing 30% sucrose at 4°C overnight. The specimens were preserved at −80°C for further use. The AS diagnosis was consistent with the new classification criteria of axial spondyloarthritis proposed by the Assessment of Spondyloarthritis International Society (Raychaudhuri and Deodhar, 2014). We collected written informed consent from all subjects prior to the study. The Ethics Committee of Xinhua Hospital Affiliated with Shanghai Jiaotong University School of Medicine approved this study (XHEC-D-076), which conformed to the principles of the Declaration of Helsinki (2013).

Chondrocyte isolation and culture

Under aseptic conditions, cartilage tissues from normal controls and AS patients were transferred into two separate culture dishes. The cartilage tissues were cut into approximately 1-mm^3 pieces, centrifuged at 1,000 rpm for 8 min and the supernatant was discarded. The sample was digested with 0.25% trypsin at 37°C for 5 min, centrifuged and resuspended in 10 ml PBS. The precipitate was added to 10 ml Dulbecco's modified Eagle's medium (DMEM)/F12 containing 0.2% collagenase II and transferred to a culture flask for incubation at 37°C and 5% CO_2 for 12 h. The cell suspension was filtered through a 200 mesh filter, and the filtrate was collected, centrifuged and the supernatant was discarded. The cells were resuspended in DMEM/F12 medium containing 10% fetal bovine serum (FBS). The cells (1×10^6 cells/ml) were inoculated in 100-mm culture dishes for incubation in 5% CO_2 at 37°C. The liquid was renewed approximately every three days. When the cells reached greater than 90% confluence, the cells were subcultured. Chondrocytes were identified by toluidine blue staining. Briefly, chondrocytes were fixed in 4% paraformaldehyde, washed, and stained with 1% toluidine blue for 30 min. After washing with double distilled water, the cells were rinsed with absolute ethanol once, dried naturally, observed and photographed under a microscope.

293T cells were obtained from American Type Culture Collection (ATCC; USA) and cultured with DMEM (Gibco, USA) containing 10% FBS (Gibco), 100 U/ml penicillin and 100 μg/ml streptomycin (Gibco).

Chondrocyte transfection

Chondrocytes were inoculated into a 6-well plate when cell confluence reached 70% 24 h before transfection. Lipofectamine 2000 (20 μl, 11668019; Thermo Fisher Scientific, USA) was used for transfection with the following plasmids (Supplementary Table S1): short hairpin RNA (shRNA) plasmid targeting MLALT1 negative control (NC) (sh-M-NC), shRNA against MALAT1#1 and MALAT1#2, MALAT1 NC overexpression vector (oe-M-NC), MALAT1 overexpression vector (oe-MALAT1), mimic NC, miR-558 mimic, inhibitor NC, miR-558 inhibitor, shRNA against GSDMD NC (sh-G-NC), shRNA targeting GSDMD#1 or GSDMD#2 (Genechem, China).

Reverse transcription quantitative polymerase chain reaction (RT-qPCR)

Total RNA extraction was performed using TRIzol reagent (Invitrogen, USA), and total RNA was subsequently reverse

transcribed to complementary DNA (cDNA) using a PrimeScript reverse transcription kit (Takara Holdings, Japan; https://www.takarabiomed.com.cn/) and cDNA reverse transcription kit (K1622; Beijing Yaanda Biotechnology, China; https://www.biomart.cn/58481/index.htm). For miRNA, a poly-A tail detection kit (B532451; Shenggong, China) was used to obtain miRNA cDNA containing a poly-A tail. RT-qPCR was performed with a SYBR® Premix Ex TaqTM II kit (Takara Holdings) using an RT-qPCR instrument (ABI7500; ABI, USA). U6 was selected as the internal reference for miR-558, and glyceraldehyde-3-phosphate dehydrogenase (GAPDH) was selected as the internal reference for the remaining factors. The primer sequences of the genes are displayed in Supplementary Table S2.

Western blot analysis

Total protein was extracted using a radioimmunoprecipitation assay kit (R0010; Beijing Solarbio Science & Technology, China), and protein concentration was determined using a bicinchoninic acid kit (20201ES76; Yeasen Biotechnology, China). After separation, the protein was transferred to a polyvinylidene fluoride membrane, which was blocked with 5% bovine serum albumin (BSA) for 1 h and incubated with diluted primary antibodies (Abcam, UK) rabbit antibodies against GSDMD (ab228824, 1:100), NLRP3 (ab214185, 1:800), and caspase-1 (ab207802, 1:1,000) at 4°C overnight. The membrane was re-probed with a secondary antibody, i.e., horseradish peroxidase (HRP)-labeled goat anti-rabbit immunoglobulin G (IgG) (1:5,000; Proteintech Group, USA), for 1 h. The membranes were developed and analyzed using Quantity One v4.6.2 software. The ratio of the gray value of the target band to GAPDH (1:5,000, 10494-1-AP; Proteintech Group) represented the relative expression of the protein.

Enzyme-linked immunosorbent assay (ELISA)

Levels of the inflammatory factor IL-1β (ab46052; Abcam) and IL-18 (ab215539; Abcam) were measured according to the manufacturer's instructions for related ELISA kits (YQ; Imunbio, China). A microplate reader (BS-1101; DeTie Laboratory Equipment, China) was used to detect the absorbance value at a wavelength of 492 nm, followed by the construction of the standard curve.

Dual-luciferase reporter gene assay

The wild-type (WT) and mutant (MUT) sequences of the 3'-UTR regions of MALAT1, miR-558, and GSDMD were synthesized artificially. The correctly sequenced WT and MUT luciferase reporter plasmids of miR-558 and GSDMD were cloned into the pmiR-RB-REPORTTM vectors (Guangzhou RiboBio, China; http://ribobio.bioon.com.cn/). NC mimic or miR-558 mimic and oe-M-NC, oe-MALAT1, or oe-MALAT1-MUT were co-transduced with the constructed luciferase reporter vectors into 293T cells. After 48 h, the cells were collected, lysed, and centrifuged for 3-5 min to obtain the supernatant. The luciferase activity was measured using the Luciferase Reporter Assay Kit (RG005; Beyotime Institute of Biotechnology, China), and firefly luciferase was used as an internal reference.

RNA-pulldown assay

Transfection was performed with 50 nM biotinylated bio-MALAT1-WT, bio-MALAT1-MUT, WT-biomiR-558, and MUT-biomiR-558 (Wuhan Genecreate Bioengineering, China). The RNA pulldown assay was performed as previously described (Xing et al., 2016).

RNA immunoprecipitation (RIP) assay

The binding of MALAT1 and miR-558 to AGO2 protein was detected using an RIP kit (Merck Millipore, USA) (Bierhoff, 2018) with rabbit anti-AGO2 (ab186733, 1:50; Abcam) and rabbit anti-IgG (ab109489, 1:100; Abcam, NC) antibodies.

Fluorescence *in situ* hybridization (FISH)

The details of the subcellular localization of lncRNA MALAT1 were obtained using a bioinformatics website (http://LNCatlas.crg.eu/), which showed that lncRNA MALAT1 was mostly localized in the nuclei of tumor cells. A FISH assay was performed based on a previous study (Soares et al., 2018). Fluorescence detection was performed under a fluorescence microscope (Olympus, Japan).

Cell counting kit-8 (CCK-8) assay

The viability of chondrocytes was assayed using a CCK-8 kit (CA1210-100; Solarbio, China). Chondrocytes in logarithmic growth phase were cultured in a 96-well plate (5×10^3 cells/well) for 3 days. Ten microliters of CCK-8 reagent was added to each well for another 2 h of culture. The absorbance value of each well was measured once every 24 h at a wavelength of 450 nm using a microplate reader.

Hoechst 33342 and propidium iodide (PI) double staining

Chondrocytes were inoculated on coverslips in 24-well plates and subsequently induced by PMA (phorbol 12-myristate 13-acetate). Each well was incubated with 4 μl Hoechst staining solution/400 μl culture solution at 37°C for 10 min. After removal of the supernatant, the cells were washed with PBS, 1 ml buffer A working fluid and 5 μl PI stain were added without light exposure for 10 min. After removal of the supernatant, the cells were washed with PBS, observed and photographed under a fluorescence microscope.

Terminal deoxyribonucleotidyl transferase dUTP nick-end labeling (TUNEL) staining

The naturally dried cell coverslips were fixed in 4% paraformaldehyde for 30 min, rinsed three times with PBS (5 min each time), and immersed in 1% Triton X-100 permeable solution for 3 min. The coverslips containing positive control cells were reacted with 100 μl DNase I reaction solution at 37°C for 30 min and washed three times with PBS (5 min each time). The cell coverslips were reacted with 50 μl TdT enzyme reaction solution at 37°C for 60 min. After rinsing three times with PBS (5 min each time), the cell coverslips were incubated with 50 μl streptavidin-TRITC solution at 37°C for 30 min. The nuclei were counterstained with 6-diamidino-2-phenylindole at room temperature for 10 min. The cells were sealed with diluted glycerol, observed and photographed under a fluorescence microscope at an excitation wavelength of 543 nm and emission wavelength of 571 nm.

Statistical analysis

Data analyses were performed using IBM SPSS Statistics software (ver. 21.0; IBM, USA). The measurement data are expressed as the mean ± SD and conformed to a normal distribution and homogeneity of variance. The unpaired *t*-test was selected for comparisons between two groups, and one-way ANOVA was used for comparisons of multiple groups, followed by Tukey's post-hoc test. The data at different time points were analyzed using repeated-measures ANOVA, and Bonferroni's test was performed for post hoc tests. Statistical significance was confirmed at $P < 0.05$.

RESULTS

LncRNA MALAT1 is upregulated in AS cartilage tissues and chondrocytes

Accumulating evidence demonstrated that MALAT1 was a competing endogenous RNA (ceRNA) that decoyed miRNA to affect the progression of diseases (Gu et al., 2017; Wang et al., 2017). Based on the AS-related dataset GSE41038, the expression of MALAT1 and GSDMD was significantly increased in AS samples compared to normal samples (Fig. 1A). RT-qPCR confirmed the highly expressed lncRNA MALAT1 in AS cartilage tissues compared to normal controls (Fig. 1B).

AS chondrocytes and normal chondrocytes were isolated and identified using inverted microscopy and toluidine blue staining. The findings showed that the isolated chondrocytes exhibited a polygonal appearance, abundant cytoplasm, clear nuclei, and round or oval nuclei located in the center of the cell body with 1-3 nucleoli. The cells had good refraction and optimal colony growth (Fig. 1C), which suggested the successful isolation and culture of chondrocytes. RT-qPCR revealed an enhancement in lncRNA MALAT1 in AS chondrocytes (Fig. 1D). These results suggested that MALAT1 expression was elevated in AS cartilage tissues and chondrocytes.

Silencing of MALAT1 promotes viability and inhibits pyroptosis of chondrocytes in AS

The functional role of lncRNA MALAT1 in the viability and pyroptosis of chondrocytes in AS was examined. FISH demonstrated that the expression of MALAT1 in the cytoplasm was markedly decreased after MALAT1 knockdown (Supplementary Fig. S1). RT-qPCR and ELISA revealed that MALAT1 knockdown reduced the levels of MALAT1, IL-1β, and IL-18, and the overexpression of MALAT1 led to opposite trends (Figs. 2A and 2B).

It was evident that the silencing of MALAT1 induced a reduction in the levels of pyroptosis-related proteins (NLRP3, caspase-1, and GSDMD), and the overexpression of MALAT1 produced the opposite trends (Fig. 2C, Supplementary Fig. S2A). Functional assays showed that MALAT1 silencing promoted cell viability but inhibited pyroptosis and apoptosis of chondrocytes, and the upregulation of MALAT1 induced opposite trends (Figs. 2D-2F, Supplementary Figs. S3A and S3B). These findings demonstrated that the depletion of MALAT1 facilitated chondrocyte viability and suppressed py-

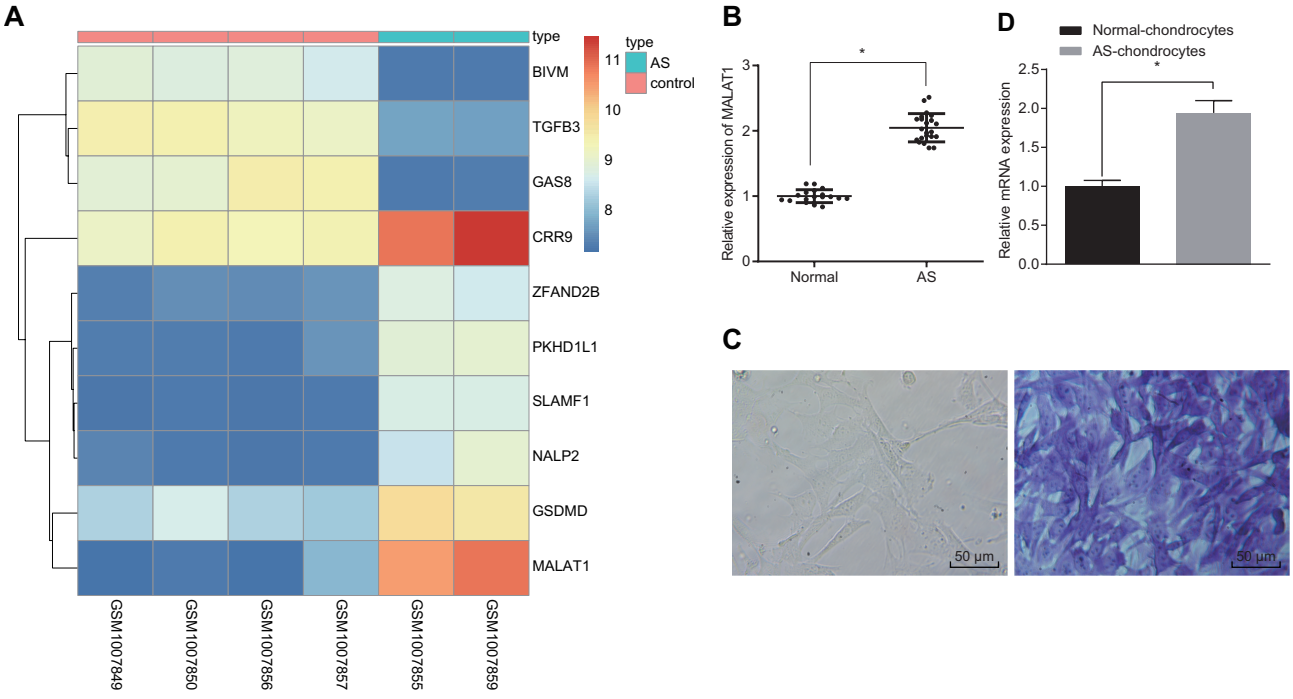

Fig. 1. LncRNA MALAT1 elevation occurs in AS cartilage tissues and chondrocytes. (A) The expression of lncRNA MALAT1 and GSDMD in the AS-related dataset GSE41038. (B) LncRNA MALAT1 expression in AS cartilage tissues and normal control cartilage tissues determined using RT-qPCR. (C) Chondrocytes identified using inverted microscopy and toluidine blue staining (×200). Scale bars = 50 μm. (D) LncRNA MALAT1 expression in normal chondrocytes and AS chondrocytes determined using RT-qPCR. *$P < 0.05$ vs normal control cartilage tissues or normal chondrocytes. All measurement data are depicted as the mean ± SD. Comparisons between two groups were performed using unpaired *t*-tests. The experiment was repeated three times (normal control cartilage tissues n = 18; AS cartilage tissues n = 22).

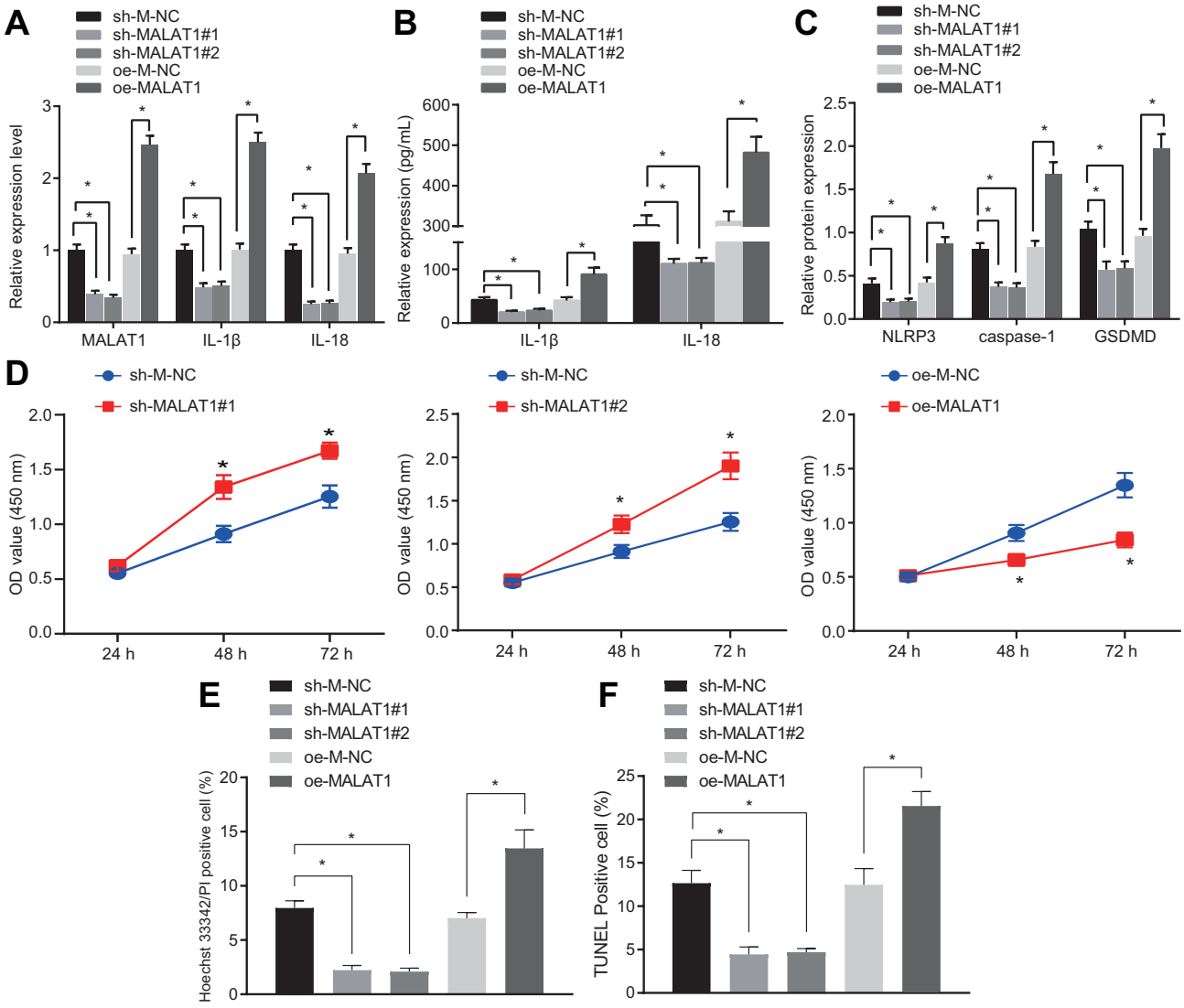

Fig. 2. Depleted lncRNA MALAT1 enhances chondrocyte viability and suppresses pyroptosis in chondrocytes. Chondrocytes were treated with restored or depleted lncRNA MALAT1. (A) The levels of lncRNA MALAT1, IL-1β, and IL-18 determined using RT-qPCR. (B) The levels of IL-1β and IL-18 measured using ELISA. (C) The protein levels of GSDMD, NLRP3, and caspase-1 determined using Western blot analysis. (D) The cell viability detected using CCK8 assay. (E) The pyroptosis detection of chondrocytes using Hoechst 33342/PI double staining. (F) Apoptosis detection of chondrocytes using TUNEL staining. $*P < 0.05$ vs AS chondrocytes treated with sh-M-NC or oe-M-NC. All measurement data are depicted as the mean ± SD. Comparisons among multiple groups were assessed using one-way ANOVA (Tukey's post-hoc test), and comparisons of data at different time points were analyzed using repeated-measures ANOVA (Bonferroni's post-hoc test). The experiment was repeated three times.

roptosis of chondrocytes and inflammation.

Upregulation of miR-558 promotes chondrocyte viability and inhibits chondrocyte pyroptosis in AS

To examine the downstream miRNAs of MALAT1, we predicted the miRNAs regulated by MALAT1 and GSDMD from the RNA22 and TargetScan websites and found that MALAT1 and GSDMD could target hsa-miR-3135b, hsa-miR-4644, hsa-miR-5192, and hsa-miR-558 (Fig. 3A). RT-qPCR was performed to determine miR-3135b, miR-4644, miR-5192, and miR-558 expression in AS cartilage tissues and normal control cartilage tissues. The results showed that miR-558 expression was the most significantly decreased in AS cartilage tissues (Fig. 3B). Decreased miR-558 expression was also observed in AS chondrocytes (Fig. 3C). These findings demonstrated that miR-558 was downregulated in AS cartilage tissues and chondrocytes.

The roles of miR-558 in the viability and pyroptosis of chondrocytes in AS were assayed. RT-qPCR and ELISA results showed that miR-558 mimic treatment inhibited the levels of IL-1β and IL-18, and miR-558 inhibitor treatment resulted in the opposite results (Figs. 3D and 3E). The restoration of miR-558 caused a reduction in the levels of NLRP3, caspase-1, and GSDMD, and the downregulation of miR-558 led to the

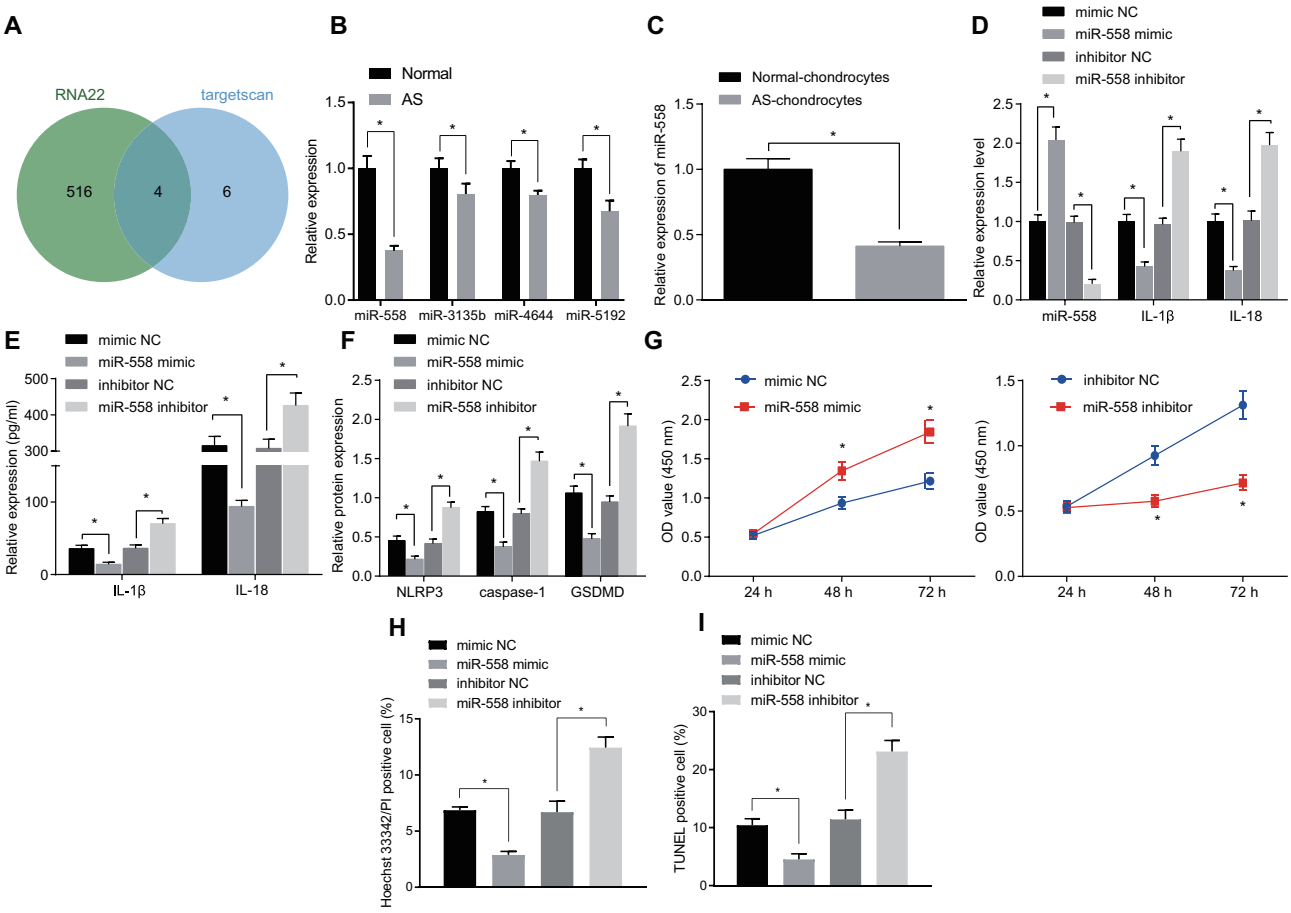

Fig. 3. Restoration of miR-558 enhances chondrocyte viability and suppresses chondrocyte pyroptosis in AS. Chondrocytes were treated with restored or depleted miR-558. (A) The downstream miRNAs of MALAT1 and GSDMD predicted by the RNA22 website (https://cm.jefferson.edu/RNA22/) and the TargetScan website (http://www.targetscan.org/vert_72/). (B) The miR-3135b, miR-4644, miR-5192, and miR-558 expression in AS cartilage tissues and normal control cartilage tissues measured using RT-qPCR. (C) The miR-558 expression in normal chondrocytes and AS chondrocytes measured using RT-qPCR. (D) The miR-558 expression and mRNA levels of IL-1β and IL-18 using RT-qPCR. (E) The levels of IL-1β and IL-18 measured using ELISA. (F) The protein levels of GSDMD, NLRP3, and caspase-1 determined using Western blot analysis. (G) The cell viability detection using CCK-8 assay. (H) The pyroptosis of chondrocytes detected using Hoechst 33342/PI double staining. (I) Apoptosis detection of chondrocytes using TUNEL staining. $*P < 0.05$ vs normal control cartilage tissues/normal chondrocytes/AS chondrocytes treated with mimic NC or inhibitor NC; All measurement data are depicted as the mean ± SD; comparisons between two groups were performed using unpaired *t*-test; comparisons of multiple groups were assessed using one-way ANOVA (Tukey's post-hoc test), and comparisons of data at different time points were analyzed using repeated-measures ANOVA (Bonferroni's post-hoc test). The experiment was repeated three times (normal control cartilage tissues n = 18; AS cartilage tissues n = 22).

opposite trends (Fig. 3F, Supplementary Fig. S2B). The overexpression of miR-558 promoted cell viability and suppressed cell pyroptosis and apoptosis (Figs. 3G-3I, Supplementary Figs. S3C and S3D). Therefore, the obtained data suggested that restoration of miR-558 effectively enhanced chondrocyte viability and suppressed chondrocyte pyroptosis in AS.

Silencing of GSDMD promotes viability and inhibits pyroptosis of chondrocytes in AS

GSDMD is a vital regulator of pyroptosis (Kayagaki et al., 2019). We focused on the underlying mechanism of GSDMD in pyroptosis of chondrocytes in AS. As shown by RT-qPCR and Western blot analyses, GSDMD was significantly increased in AS cartilage tissues (Figs. 4A and 4B, Supplementary Fig. S2C). Elevated mRNA levels of GSDMD were also found in AS chondrocytes (Fig. 4C).

The roles of GSDMD in the viability and pyroptosis of chondrocytes in AS were further examined. AS chondrocytes were treated with sh-G-NC, sh-GSDMD#1, or sh-GSDMD#2 plasmids. RT-qPCR determination and ELISA revealed that the levels of IL-1β and IL-18 were significantly reduced after the knockdown of GSDMD (Figs. 4D and 4E). Western blot analysis revealed that the protein levels of NLRP3 and caspase-1 were significantly decreased after the downregulation of GSDMD (Fig. 4F, Supplementary Fig. S2D). The downregulation of GSDMD promoted chondrocyte viability and sup-

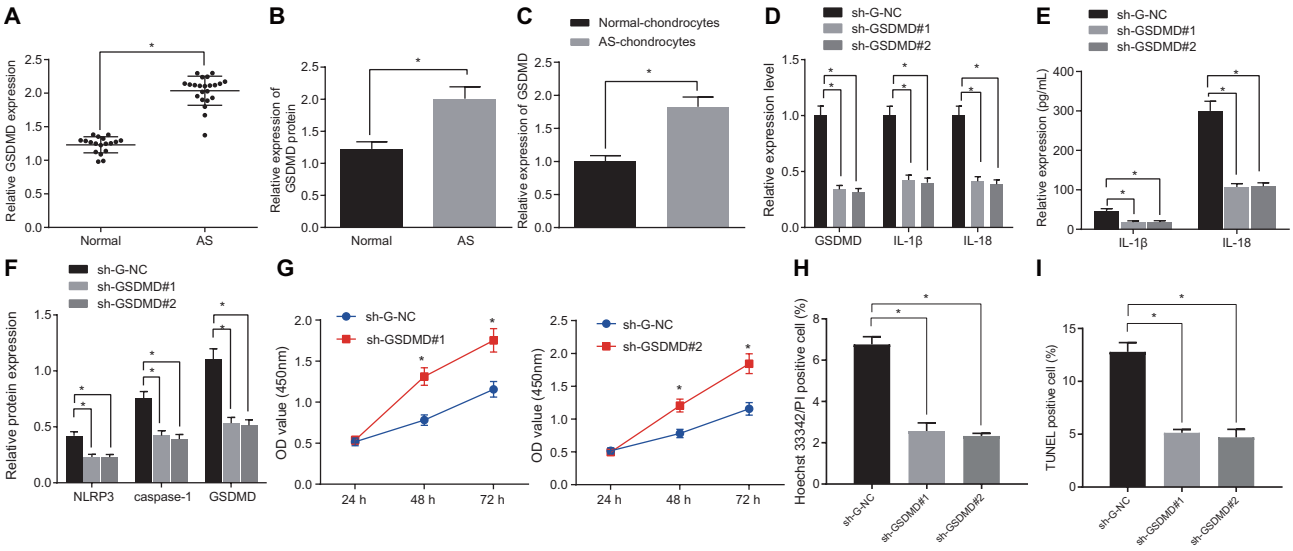

Fig. 4. Depleted GSDMD enhances chondrocyte viability and suppresses pyroptosis of chondrocytes. Chondrocytes were treated with depleted GSDMD. (A) The mRNA level of GSDMD in AS cartilage tissues and normal control cartilage tissues measured using RT-qPCR. (B) The protein level of GSDMD in AS cartilage tissues and normal control cartilage tissues measured using Western blot analysis. (C) The mRNA level of GSDMD in normal chondrocytes and AS chondrocytes measured using RT-qPCR. (D) The mRNA levels of GSDMD, IL-1β, and IL-18 determined using RT-qPCR. (E) The levels of IL-1β and IL-18 measured using ELISA. (F) The protein levels of GSDMD, NLRP3, and caspase-1 determined using Western blot analysis. (G) Cell viability detected using CCK-8 assay. (H) The pyroptosis of chondrocytes detected using Hoechst 33342/PI double staining. (I) Apoptosis detection of chondrocytes using TUNEL staining. $*P < 0.05$ vs normal control cartilage tissues/normal chondrocytes/AS chondrocytes treated with sh-G-NC. All measurement data are depicted as the mean ± SD. Comparisons between two groups were performed using unpaired *t*-tests. Comparisons between multiple groups were assessed using one-way ANOVA (Tukey's post-hoc test), and comparisons of data at different time points were analyzed using repeated-measures ANOVA (Bonferroni's post-hoc test). The experiment was repeated three times (normal control cartilage tissues n = 18; AS cartilage tissues n = 22).

pressed chondrocyte pyroptosis and apoptosis (Figs. 4G-4I, Supplementary Figs. S3E and S3F). Collectively, the silencing of GSDMD promoted viability and inhibited pyroptosis of chondrocytes in AS.

LncRNA MALAT1 competitively binds to miR-558 to regulate GSDMD expression

Blast analysis predicted a binding site between MALAT1 and miR-558 (Fig. 5A), which was further validated using a dual-luciferase assay. The luciferase activity of WT-miR-558/oe-MALAT1 was inhibited compared to the cells treated with oe-M-NC plasmids, but no alteration was seen after oe-MALAT1-MUT (Fig. 5B). As shown in Fig. 5C, the specific adsorption level of Ago2 by MALAT1 and miR-588 was significantly increased. Relative to Bio-probe NC, the enrichment of MALAT1 in the cells treated with Bio-miR-558-WT was enhanced, but no obvious difference was found in cells treated with Bio-miR-558-MUT. Compared to the Bio-probe NC group, the enrichment level of miR-558 in the Bio-MALAT1-WT group was significantly increased, and the enrichment level of miR-558 in the Bio-MALAT1-MUT group was not significantly different (Fig. 5D). These findings suggested that lncRNA MALAT1 acted as a ceRNA to sponge miR-558 and affect miR-558 expression.

The prediction from TargetScan suggested binding sites between miR-558 and GSDMD (Fig. 5E), which was validated in the dual-luciferase assay (Fig. 5F). We speculated that MALAT1 functioned as a ceRNA of miR-558 to inhibit miR-558 expression and increase GSDMD expression. To verify this hypothesis, cells were treated with restored or depleted MALAT1 and/or miR-558. We found that knockdown of MALAT1 increased the expression of miR-558 and inhibited GSDMD expression, and the upregulation of MALAT1 produced the opposite trends (Fig. 5G).

Cells were treated with oe-MALAT1 + mimic NC, oe-MALAT1 + miR-558 mimic, sh-MALAT1 + inhibitor NC, sh-MALAT1 + miR-558 inhibitor, miR-558 inhibitor + sh-G-NC, and miR-558 inhibitor + sh-GSDMD. RT-qPCR (Fig. 5H) showed that the expression of MALAT1 and GSDMD was significantly decreased after the additional treatment with the miR-558 mimic compared to cells treated with oe-MALAT1 alone. sh-MALAT1 in combination with an miR-558 inhibitor increased the expression of MALAT1 and GSDMD compared to sh-MALAT1 treatment alone. sh-GSDMD exhibited no significant difference in the expression of MALAT1 and miR-558 but GSDMD expression was remarkably reduced in miR-558 inhibitor-treated cells. Therefore, the obtained data suggested that MALAT1 inhibited miR-558 expression by binding to miR-558 and increase GSDMD expression, and the knockdown of MALAT1 or the upregulation of miR-558 inhibited GSDMD expression.

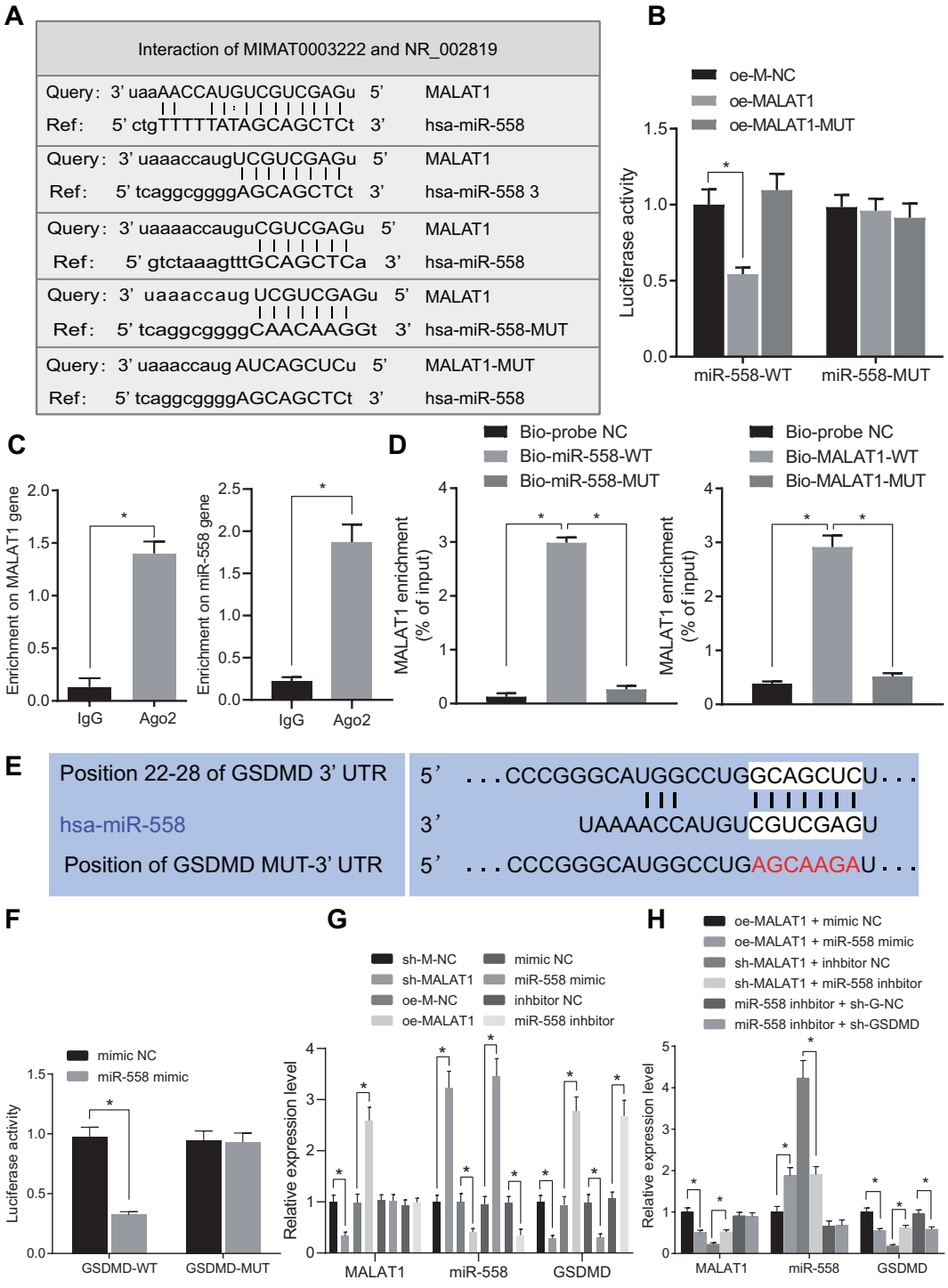

Fig. 5. LncRNA MALAT1 competitively binds to miR-558 to promote GSDMD expression. (A) The binding sites between lncRNA MALAT1 and miR-558 predicted using Blast. (B) The relationship between lncRNA MALAT1 and miR-558 verified by dual-luciferase reporter gene assay. (C) The binding of lncRNA MALAT1 and miR-558 to Ago2 detected using the RIP assay. (D) The binding of lncRNA MALAT1 to miR-558 analyzed using the RNA-pull down assay. (E) The binding sites between miR-558 and GSDMD predicted using TargetScan. (F) The relationship between miR-558 and GSDMD verified by dual-luciferase reporter gene assay. (G) The expression of miR-558, and GSDMD determined using RT-qPCR. (H) The expression of lncRNA MALAT1, miR-558, and GSDMD determined using RT-qPCR. $*P < 0.05$ vs the oe-M-NC group, IgG group, Bio-probe NC group, mimic NC group, AS-chondrocytes treated with sh-M-NC, oe-M-NC, mimic NC or inhibitor NC. All measurement data are depicted as the mean ± SD. Comparisons between two groups were performed using unpaired *t*-tests. Comparisons between multiple groups were assessed using one-way ANOVA (Tukey's post-hoc test). The experiment was repeated three times.

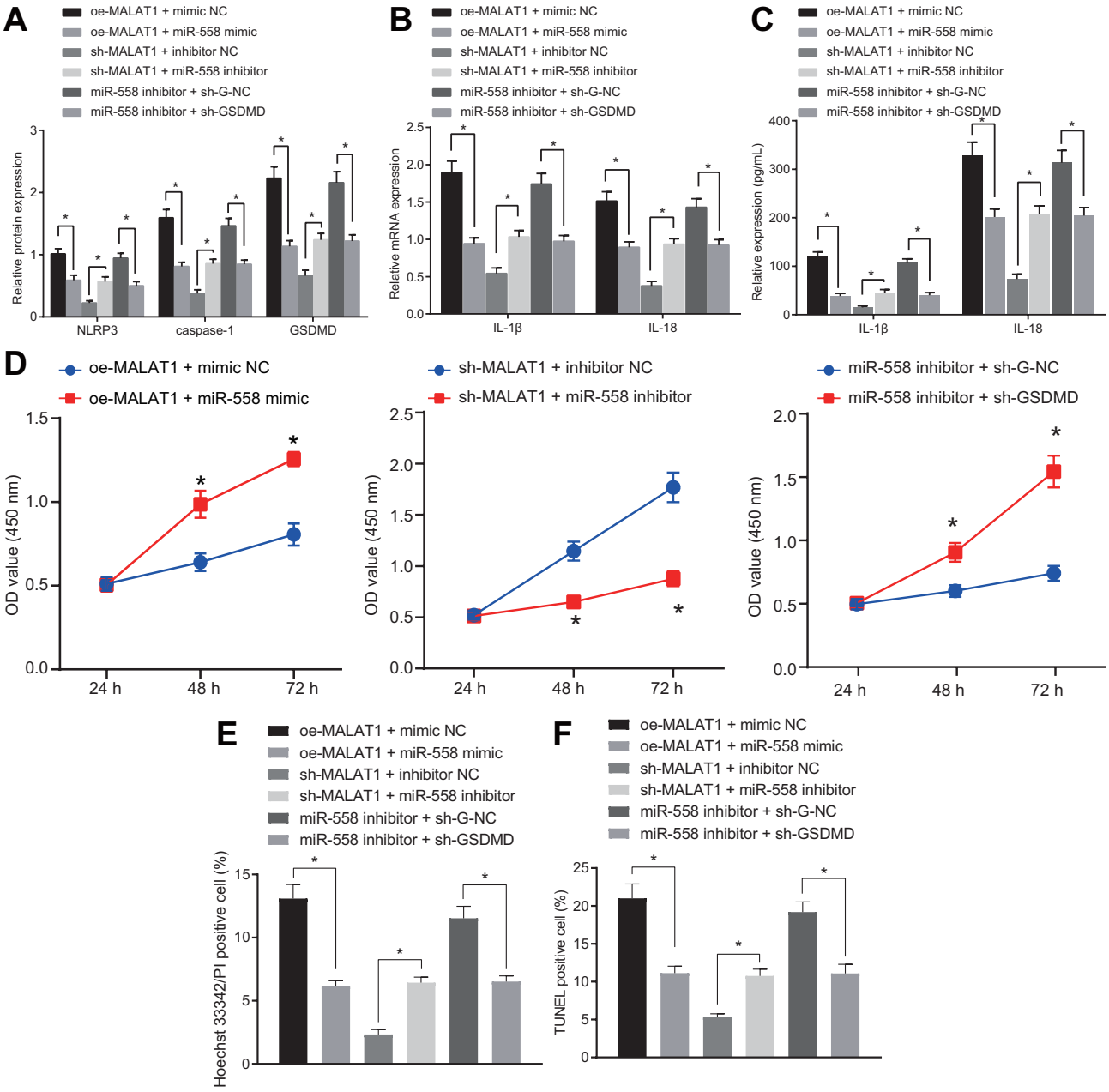

Fig. 6. Silencing of lncRNA MALAT1 increases miR-558 to promote viability and inhibit apoptosis and pyroptosis of chondrocytes in AS via inhibition of GSDMD expression. Chondrocytes were treated with restored or depleted lncRNA MALAT1 and/or miR-558. (A) The protein levels of GSDMD, NLRP3, and caspase-1 measured using Western blot analysis. (B) The mRNA levels of IL-1β and IL-18 determined using RT-qPCR. (C) The levels of IL-1β and IL-18 measured using ELISA. (D) Cell viability detected using CCK-8 assay. (E) The pyroptosis of chondrocytes detected using Hoechst 33342/PI double staining. (F) The apoptosis of chondrocytes detected using TUNEL staining. $*P < 0.05$ vs cells treated with oe-MALAT1 + mimic NC, sh-MALAT1 + inhibitor NC or miR-558 inhibitor + sh-G-NC. All measurement data are depicted as the mean ± SD. Comparisons between multiple groups were assessed using one-way ANOVA (Tukey's post-hoc test), and comparisons of data at different time points were analyzed using repeated-measures ANOVA (Bonferroni post-hoc test). The experiment was repeated three times.

Silencing of lncRNA MALAT1 suppresses the ability of miR-558 to inhibit chondrocyte pyroptosis in AS by inhibiting GSDMD

We further identified the effects of MALAT1 regulation of GSDMD expression via binding to miR-558 on the progression of AS. As shown by Western blot, RT-qPCR and ELISA (Figs. 6A-6C, Supplementary Fig. S2E), additional treatment with the miR-558 mimic contributed to a significant decrease in NLRP3, caspase-1, and GSDMD protein levels and IL-1β and IL-18 levels in the cells treated with oe-MALAT1. The

miR-558 inhibitor triggered a remarkable increase in the protein levels of NLRP3, caspase-1, and GSDMD and IL-1β and IL-18 after MALAT1 knockdown in cells. Compared to miR-558 inhibitor treatment alone, the protein levels of NLRP3 and caspase-1 and IL-1β and IL-18 were diminished after the combination of miR-558 inhibitor and sh-GSDMD.

Compared to cells treated with oe-MALAT1 alone, cells treated with oe-MALAT1 and miR-558 mimic in combination had increased cell viability and decreased apoptosis and pyroptosis of chondrocytes. Additional treatment with the miR-558 inhibitor suppressed cell viability and enhanced apoptosis and pyroptosis of chondrocytes in the presence of sh-MALAT1. Knockdown of GSDMD promoted cell viability and inhibited apoptosis and pyroptosis of chondrocytes in the cells treated with the miR-558 inhibitor (Figs. 6D-6F, Supplementary Figs. S3G and S3H). Taken together, the silencing of MALAT1 contributed to the increase in miR-558 to suppress GSDMD expression and facilitate cell viability and inhibit inflammation, apoptosis and pyroptosis of chondrocytes in AS.

DISCUSSION

LncRNAs act as ceRNAs of miRNAs to exert effects on AS (Zhang et al., 2017). The present study focused on the underlying mechanism of the lncRNA MALAT1 in AS and its related ceRNA activity. Our cell experiments showed that silencing lncRNA MALAT1 increased miR-558 by suppressing GSDMD expression to promote cell viability and inhibit apoptosis and pyroptosis of chondrocytes in AS.

Initial findings from our investigation showed that lncRNA MALAT1 and GSDMD were highly expressed and miR-558 was poorly expressed in AS cartilage tissues and chondrocytes. Accumulating evidence suggested that aberrant expression of lncRNAs was involved in various kinds of cancers (Adams et al., 2017; Bhan et al., 2017) and the in ammation and progression of pathological osteogenesis in AS (Xie et al., 2016). Zhou et al. (2018) suggested that lncRNA MALAT1 expression was obviously increased in the spinal cord of rats following spinal cord injury. A total of 196 lncRNAs were upregulated and 16 miRNAs, such as miR-27b-3p, were downregulated in patients with AS (Zhang et al., 2017). The bioinformatics prediction revealed potential binding sites between lncRNA MALAT1 and miR-558, which suggests a possible interaction. Consistent with our findings, changes in the expression profile of miRNAs were also found in some autoimmune diseases, such as AS (Mohammadi et al., 2018). The expression of miRNAs, such as miR-16, miR-221, and let-7i, is dysregulated in patients with AS (Lai et al., 2013). A recent study found that miR-558 was poorly expressed in human OA chondrocytes (Park et al., 2013). The present study demonstrated that miR-558 targeted GSDMD. GSDMD is a new element of in ammasomes that is required for pyroptosis and IL-1β secretion (He et al., 2015). The upregulation of GSDMD was also demonstrated in the liver tissues of patients with non-alcoholic steatohepatitis (Xu et al., 2018). This evidence suggests that the MALAT1/miR-558/GSDMD axis plays a key role in the progression of AS.

The present study also found that the depletion of lncRNA MALAT1 expression contributed to the increase of miR-558, enhanced cell viability, reduced levels of IL-1β and IL-18, and suppressed apoptosis and pyroptosis of chondrocytes in AS via inhibition of GSDMD. A previous study demonstrated that inflammation was characterized by the stimulation of pyroptosis and release of IL-1β and IL-18 (Lamkanfi and Dixit, 2014). The downregulation of lncRNA MALAT1 hindered the inflammation of microglial cells to relieve the progression of acute spinal cord injury (Zhou et al., 2018). Depletion of lncRNA MALAT1 suppressed pyroptosis in HK-2 cells via the overexpression of miR-23c (Li et al., 2017). Notably, miRNAs are highly important in the regulation of the immune response and the development of immune cells (Nejad et al., 2018). A study reported that the reduced expression of miR-558 was related to the activation of IL-1β (Park et al., 2013). GSDMD often leads to the secretion of mature cytokines, including IL-1β and IL-18, which recruit more immune cells to trigger inflammation, and support GSDMD as a crucial inflammatory regulator (Yang et al., 2018). GSDMD depletion reduced the induction of pyroptosis to inhibit the inflammatory reaction (Shi et al., 2015). These prior reports provide insights into the mechanisms underlying the lncRNA MALAT1/miR-558/GSDMD axis, which contributes to the reduction in IL-1β and IL-18 levels. Ultimately, these alterations may stimulate cell viability and inhibit inflammatory responses, apoptosis and pyroptosis of chondrocytes in AS.

In conclusion, the down-regulation of lncRNA MALAT1 decreased miR-558-mediated GSDMD expression to enhance cell viability and suppress apoptosis and pyroptosis of chondrocytes in AS. Our results elucidate the underlying mechanisms of AS and provide a marker for AS treatment in the future.

Note: Supplementary information is available on the Molecules and Cells website (www.molcells.org).

AUTHOR CONTRIBUTIONS

W.C. and F.W. designed the study. J.W. and F.C. collated the data, carried out data analyses and produced the initial draft of the manuscript. T.C. contributed to drafting the manuscript. All authors have read and approved the final submitted manuscript.

CONFLICT OF INTEREST

The authors have no potential conflicts of interest to disclose.

ORCID

Wei Chen https://orcid.org/0000-0003-3131-7257
Feilong Wang https://orcid.org/0000-0003-4067-7668
Jiangtao Wang https://orcid.org/0000-0001-8259-0232
Fuyu Chen https://orcid.org/0000-0003-0945-6381
Ting Chen https://orcid.org/0000-0001-8631-9351

REFERENCES

Adams, B.D., Parsons, C., Walker, L., Zhang, W.C., and Slack, F.J. (2017). Targeting noncoding RNAs in disease. J. Clin. Invest. *127*, 761-771.

Bhan, A., Soleimani, M., and Mandal, S.S. (2017). Long noncoding RNA and cancer: a new paradigm. Cancer Res. *77*, 3965-3981.

Bierhoff, H. (2018). Analysis of lncRNA-protein interactions by RNA-

protein pull-down assays and RNA immunoprecipitation (RIP). Methods Mol. Biol. *1686*, 241-250.

Garcia-Montoya, L., Gul, H., and Emery, P. (2018). Recent advances in ankylosing spondylitis: understanding the disease and management. F1000Res. *7*, F1000 Faculty Rev-1512.

Gu, Y., Xiao, X., and Yang, S. (2017). LncRNA MALAT1 acts as an oncogene in multiple myeloma through sponging miR-509-5p to modulate FOXP1 expression. Oncotarget *8*, 101984-101993.

Guo, X., Wu, X., Han, Y., Tian, E., and Cheng, J. (2019). LncRNA MALAT1 protects cardiomyocytes from isoproterenol-induced apoptosis through sponging miR-558 to enhance ULK1-mediated protective autophagy. J. Cell. Physiol. *234*, 10842-10854.

Han, Y., Qiu, H., Pei, X., Fan, Y., Tian, H., and Geng, J. (2018). Low-dose sinapic acid abates the pyroptosis of macrophages by downregulation of lncRNA-MALAT1 in rats with diabetic atherosclerosis. J. Cardiovasc. Pharmacol. *71*, 104-112.

He, D., Zheng, J., Hu, J., Chen, J., and Wei, X. (2020). Long non-coding RNAs and pyroptosis. Clin. Chim. Acta *504*, 201-208.

He, W.T., Wan, H., Hu, L., Chen, P., Wang, X., Huang, Z., Yang, Z.H., Zhong, C.Q., and Han, J. (2015). Gasdermin D is an executor of pyroptosis and required for interleukin-1beta secretion. Cell Res. *25*, 1285-1298.

Huang, D., Liu, J., Wan, L., Fang, Y., Long, Y., Zhang, Y., and Bao, B. (2021). Identification of lncRNAs associated with the pathogenesis of ankylosing spondylitis. BMC Musculoskelet. Disord. *22*, 272.

Kayagaki, N., Lee, B.L., Stowe, I.B., Kornfeld, O.S., O'Rourke, K., Mirrashidi, K.M., Haley, B., Watanabe, C., Roose-Girma, M., Modrusan, Z., et al. (2019). IRF2 transcriptionally induces GSDMD expression for pyroptosis. Sci. Signal. *12*, eaax4917.

Lai, N.S., Yu, H.C., Chen, H.C., Yu, C.L., Huang, H.B., and Lu, M.C. (2013). Aberrant expression of microRNAs in T cells from patients with ankylosing spondylitis contributes to the immunopathogenesis. Clin. Exp. Immunol. *173*, 47-57.

Lamkanfi, M. and Dixit, V.M. (2014). Mechanisms and functions of inflammasomes. Cell *157*, 1013-1022.

Li, H., Yang, H.H., Sun, Z.G., Tang, H.B., and Min, J.K. (2019). Whole-transcriptome sequencing of knee joint cartilage from osteoarthritis patients. Bone Joint Res. *8*, 290-303.

Li, X., Zeng, L., Cao, C., Lu, C., Lian, W., Han, J., Zhang, X., Zhang, J., Tang, T., and Li, M. (2017). Long noncoding RNA MALAT1 regulates renal tubular epithelial pyroptosis by modulated miR-23c targeting of ELAVL1 in diabetic nephropathy. Exp. Cell Res. *350*, 327-335.

Liu, C., Zhuo, H., Ye, M.Y., Huang, G.X., Fan, M., and Huang, X.Z. (2020). LncRNA MALAT1 promoted high glucose-induced pyroptosis of renal tubular epithelial cell by sponging miR-30c targeting for NLRP3. Kaohsiung J. Med. Sci. *36*, 682-691.

Liu, X. and Lieberman, J. (2017). A mechanistic understanding of pyroptosis: the fiery death triggered by invasive infection. Adv. Immunol. *135*, 81-117.

McKenzie, B.A., Dixit, V.M., and Power, C. (2020). Fiery cell death: pyroptosis in the central nervous system. Trends Neurosci. *43*, 55-73.

Mohammadi, H., Hemmatzadeh, M., Babaie, F., Gowhari Shabgah, A., Azizi, G., Hosseini, F., Majidi, J., and Baradaran, B. (2018). MicroRNA implications in the etiopathogenesis of ankylosing spondylitis. J. Cell. Physiol. *233*, 5564-5573.

Nejad, C., Stunden, H.J., and Gantier, M.P. (2018). A guide to miRNAs in inflammation and innate immune responses. FEBS J. *285*, 3695-3716.

Park, S.J., Cheon, E.J., and Kim, H.A. (2013). MicroRNA-558 regulates the expression of cyclooxygenase-2 and IL-1beta-induced catabolic effects in human articular chondrocytes. Osteoarthritis Cartilage *21*, 981-989.

Puthanveetil, P., Chen, S., Feng, B., Gautam, A., and Chakrabarti, S. (2015). Long non-coding RNA MALAT1 regulates hyperglycaemia induced inflammatory process in the endothelial cells. J. Cell. Mol. Med. *19*, 1418-1425.

Raychaudhuri, S.P. and Deodhar, A. (2014). The classification and diagnostic criteria of ankylosing spondylitis. J. Autoimmun. *48-49*, 128-133.

Shi, J., Zhao, Y., Wang, K., Shi, X., Wang, Y., Huang, H., Zhuang, Y., Cai, T., Wang, F., and Shao, F. (2015). Cleavage of GSDMD by inflammatory caspases determines pyroptotic cell death. Nature *526*, 660-665.

Soares, R.J., Maglieri, G., Gutschner, T., Diederichs, S., Lund, A.H., Nielsen, B.S., and Holmstrom, K. (2018). Evaluation of fluorescence in situ hybridization techniques to study long non-coding RNA expression in cultured cells. Nucleic Acids Res. *46*, e4.

Tay, Y., Rinn, J., and Pandolfi, P.P. (2014). The multilayered complexity of ceRNA crosstalk and competition. Nature *505*, 344-352.

Wang, Y., Zhang, Y., Yang, T., Zhao, W., Wang, N., Li, P., Zeng, X., and Zhang, W. (2017). Long non-coding RNA MALAT1 for promoting metastasis and proliferation by acting as a ceRNA of miR-144-3p in osteosarcoma cells. Oncotarget *8*, 59417-59434.

Wenker, K.J. and Quint, J.M. (2021). Ankylosing spondylitis. In StatPearls [Internet], B. Abai, ed. (Treasure Island: StatPearls Publishing).

Xi, Y., Jiang, T., Chaurasiya, B., Zhou, Y., Yu, J., Wen, J., Shen, Y., Ye, X., and Webster, T.J. (2019). Advances in nanomedicine for the treatment of ankylosing spondylitis. Int. J. Nanomedicine *14*, 8521-8542.

Xie, Z., Li, J., Wang, P., Li, Y., Wu, X., Wang, S., Su, H., Deng, W., Liu, Z., Cen, S., et al. (2016). Differential expression profiles of long noncoding RNA and mRNA of osteogenically differentiated mesenchymal stem cells in ankylosing spondylitis. J. Rheumatol. *43*, 1523-1531.

Xing, Z., Lin, C., and Yang, L. (2016). LncRNA pulldown combined with mass spectrometry to identify the novel lncRNA-associated proteins. Methods Mol. Biol. *1402*, 1-9.

Xu, B., Jiang, M., Chu, Y., Wang, W., Chen, D., Li, X., Zhang, Z., Zhang, D., Fan, D., Nie, Y., et al. (2018). Gasdermin D plays a key role as a pyroptosis executor of non-alcoholic steatohepatitis in humans and mice. J. Hepatol. *68*, 773-782.

Yang, J., Liu, Z., Wang, C., Yang, R., Rathkey, J.K., Pinkard, O.W., Shi, W., Chen, Y., Dubyak, G.R., Abbott, D.W., et al. (2018). Mechanism of gasdermin D recognition by inflammatory caspases and their inhibition by a gasdermin D-derived peptide inhibitor. Proc. Natl. Acad. Sci. U. S. A. *115*, 6792-6797.

Zhang, C., Wang, C., Jia, Z., Tong, W., Liu, D., He, C., Huang, X., and Xu, W. (2017). Differentially expressed mRNAs, lncRNAs, and miRNAs with associated co-expression and ceRNA networks in ankylosing spondylitis. Oncotarget *8*, 113543-113557.

Zhou, H.J., Wang, L.Q., Wang, D.B., Yu, J.B., Zhu, Y., Xu, Q.S., Zheng, X.J., and Zhan, R.Y. (2018). Long noncoding RNA MALAT1 contributes to inflammatory response of microglia following spinal cord injury via the modulation of a miR-199b/IKKbeta/NF-kappaB signaling pathway. Am. J. Physiol. Cell Physiol. *315*, C52-C61.